

Correlation Energies in Distorted $3d-t_{2g}$ Perovskite Oxides

I. V. Solovyev[†]

*Computational Materials Science Center (CMSC),
National Institute for Materials Science (NIMS),
1-2-1 Sengen, Tsukuba, Ibaraki 305-0047, Japan*

Using an effective low-energy Hamiltonian derived from the first-principles electronic structure calculations for the narrow t_{2g} bands of YTiO_3 , LaTiO_3 , YVO_3 , and LaVO_3 , we evaluate the contributions of the correlation energy (E_C) to the stability of different magnetic structures, which can be realized in these distorted perovskite oxides. We consider two approximations for E_C , which are based on the regular perturbation theory expansion around a nondegenerate Hartree-Fock ground state. One is the second order of perturbation theory, which allows us to compare the effects of local and nonlocal correlations. Another one is the local t -matrix approach, which allows us to treat some higher-order contributions to E_C . The correlation effects systematically improve the agreement with the experimental data and additionally stabilize the experimentally observed G - and C -type antiferromagnetic (AFM) structures in YVO_3 and LaVO_3 , though the absolute magnitude of the stabilization energy is sensitive to the level of approximations and somewhat smaller in the t -matrix method. The nonlocal correlations additionally stabilize the ferromagnetic ground state in YTiO_3 and the C -type AFM ground state in LaVO_3 . Amongst two inequivalent transition-metal sites in the monoclinic structure, the local correlations are stronger at the sites with the least distorted environment. Limitations of the regular perturbation-theory expansion for LaTiO_3 are also discussed.

PACS: 71.10.-w; 71.15.Nc; 71.28.+d; 75.25.+z

1. Introduction

An interest to the transition-metal perovskite oxides YTiO_3 , LaTiO_3 , YVO_3 , and LaVO_3 is mainly related with the variety of magnetic structures, which can be realized in these, seemingly alike, compounds. For example, YTiO_3 has the ferromagnetic (F) structure [1]. LaTiO_3 is a three-dimensional (G -type) antiferromagnet [2]. At the low temperature, YVO_3 forms the G -type antiferromagnetic (AFM) structure, which can be transformed to a chainlike (C -type) antiferromagnetic structure at around 77 K [3]. On the contrary, LaVO_3 is the C -type antiferromagnet in the whole temperature range below the magnetic transition temperature [4]. Surprisingly, the difference exists not only between titanates (YTiO_3 and LaTiO_3) and vanadites (YVO_3 and LaVO_3), which have a different number of valent electrons, but also within each group of formally isoelectronic materials. The differences are apparently related with the tiny changes in the distorted perovskite structure, which are amplified by the effects of Coulomb correlations in the narrow t_{2g} band. The details of the crystal structure can be found in Refs. [1, 2, 3, 4]. Briefly, both titanites have an orthorhombic structure, although the details of this structure are

[†]e-mail: solovyev.igor@nims.go.jp

rather different for YTiO_3 and LaTiO_3 . LaVO_3 is crystallized in a monoclinic structure. The low-temperature phase of YVO_3 is orthorhombic (shown in Fig. 1), which becomes monoclinic at around 77 K. The structural orthorhombic-monoclinic transition coincides with the G - C AFM transition. Generally, Y-based compounds are more distorted (due to smaller size of the Y^{3+} ions).

There is a large number of theoretical articles devoted to the origin of the magnetic ground states in the distorted t_{2g} perovskite oxides. The problem has been considered on the basis of first-principles electronic structure calculations (e.g., Refs. [5]) and the model approaches for the strongly-correlated systems (e.g., Refs. [6, 7, 8]). The model theories typically vary on the assessment of the role played by the lattice distortions [6] and the Coulomb correlations [7, 8].

We believe that any realistic theoretical description of these compounds is practically impossible without the impact from the first-principles electronic structure calculations: simply, the lattice distortion is too complex, and, had we try to postulate a model Hamiltonian for these t_{2g} perovskite oxides, we would inevitably face the problem of choosing the values for a large number of model parameters, which cannot be fixed in unbiased way. However, the conventional electronic structure calculations are also far from being perfect. Typically, they are supplemented with some additional approximations, which have serious limitations for treating the Coulomb correlations in the case of strongly-correlated materials. A typical example is the local-density approximation (LDA). From this point of view, a promising direction is to make a bridge between first-principles electronic structure calculations and models for the strongly-correlated systems, and construct an appropriate model Hamiltonian entirely “from the first principles”. Fortunately, in the case of transition-metal oxides, we are typically dealing only with a small group of states located near the Fermi level and well separated from the remaining part of the spectrum (for instance, t_{2g} bands in Fig. 1). These states are mainly responsible for the electronic and magnetic properties of oxide materials. Therefore, in many cases it is sufficient to consider a minimal model, consisting of only the t_{2g} bands, and include the effect of other bands into the renormalization of interaction parameters in the t_{2g} band. Such a strategy was pursued in Refs. [9, 10, 11]. It consists of three major steps: first-principles electronic structure calculations \rightarrow construction of the model Hamiltonian \rightarrow solution of this model Hamiltonian. The first applications to the distorted t_{2g} perovskite oxides have been considered in Refs. [11, 12]. The present paper deals with the last part of the problem. We will solve the model Hamiltonian derived in Ref. [11], and mainly focus on the role played by the correlation effects, beyond the mean-field Hartree-Fock (HF) approximation. Particularly, we will consider two perturbative approaches. One is the regular second-order perturbation theory for the correlation energy [13], and the other one is the t -matrix approach [14, 15, 16]. In both approaches, the HF approximation is used as the starting point. This implies that the degeneracy of the HF ground state is already lifted by the crystal distortion so that the regular perturbation theory is justified. We will also discuss some limitations of this treatment for LaTiO_3 .

2. Construction of model Hamiltonian

Our first goal is the construction of the effective multi-orbital Hubbard model for the isolated t_{2g} bands:

$$\hat{\mathcal{H}} = \sum_{\mathbf{R}\mathbf{R}'} \sum_{\alpha\beta} h_{\mathbf{R}\mathbf{R}'}^{\alpha\beta} \hat{c}_{\mathbf{R}\alpha}^\dagger \hat{c}_{\mathbf{R}'\beta} + \frac{1}{2} \sum_{\mathbf{R}} \sum_{\alpha\beta\gamma\delta} U_{\alpha\beta\gamma\delta} \hat{c}_{\mathbf{R}\alpha}^\dagger \hat{c}_{\mathbf{R}\gamma}^\dagger \hat{c}_{\mathbf{R}\beta} \hat{c}_{\mathbf{R}\delta}, \quad (1)$$

where $\hat{c}_{\mathbf{R}\alpha}^\dagger$ ($\hat{c}_{\mathbf{R}\alpha}$) creates (annihilates) an electron in the Wannier orbital $\tilde{W}_{\mathbf{R}}^\alpha$ of the transition-metal site \mathbf{R} , and α is a joint index, incorporating all remaining (spin and orbital) degrees of freedom. The matrix $\hat{h}_{\mathbf{R}\mathbf{R}'} = \|h_{\mathbf{R}\mathbf{R}'}^{\alpha\beta}\|$ parameterizes the kinetic energy of electrons, where the site-diagonal part ($\mathbf{R}=\mathbf{R}'$) describes the local level-splitting, caused by the crystal field, and the off-diagonal part ($\mathbf{R}\neq\mathbf{R}'$) stands for the transfer integrals. $U_{\alpha\beta\gamma\delta} = \int d\mathbf{r} \int d\mathbf{r}' \tilde{W}_{\mathbf{R}}^{\alpha\dagger}(\mathbf{r}) \tilde{W}_{\mathbf{R}}^\beta(\mathbf{r}) v_{\text{scr}}(\mathbf{r}-\mathbf{r}') \tilde{W}_{\mathbf{R}}^{\gamma\dagger}(\mathbf{r}') \tilde{W}_{\mathbf{R}}^\delta(\mathbf{r}') \equiv \langle \alpha\gamma | v_{\text{scr}} | \beta\delta \rangle$ are the matrix elements of *screened* Coulomb interaction $v_{\text{scr}}(\mathbf{r}-\mathbf{r}')$, which are supposed to be diagonal with respect to the site indices. In principles, $U_{\alpha\beta\gamma\delta}$ can also depend on the site-index \mathbf{R} . Nevertheless, for the sake of simplicity of our notations, here and throughout in this paper we drop the index \mathbf{R} in the notation of the Coulomb matrix elements (however, we do consider this dependence in all our calculations).

The procedure of mapping of the first-principles electronic structure calculations onto the model Hamiltonian (1) for distorted perovskite oxides has been discussed in details in Refs. [10, 11]. Here, we only outline the main idea. The kinetic-energy part, $\hat{h}_{\mathbf{R}\mathbf{R}'}$, can be obtained using the downfolding method, which is exact and equivalent to the projector-operator method [17]. The Wannier functions can be formally derived from $\hat{h}_{\mathbf{R}\mathbf{R}'}$, using the ideas of the linear-muffin-tin-orbital (LMTO) method [10, 18]. The matrix of screened Coulomb interactions in the t_{2g} band can be calculated using a hybrid approach, which combines the constraint density-functional theory with the random-phase approximation for the hybridization effects between transition-metal d and other atomic states [10]. The values of the model parameters obtained in such a way can be found in Ref. [11].

3. Solution of model Hamiltonian

3.1. Hartree-Fock approximation

The HF method provides the simplest approximation for the solution of the many-electron problem with the Hamiltonian (1). In this case, the trial many-electron wavefunction is searched in the form of a single Slater determinant $|S\{\varphi_k\}\rangle$, constructed from the one-electron orbitals $\{\varphi_k\}$. In these notations, k is a joint index, which contains the information about the momentum (\mathbf{k}) in the first Brillouin zone, the number of band (n), and the spin ($\sigma = \uparrow$ or \downarrow) of the particle. The one-electron orbitals $\{\varphi_k\}$ are subjected to the variational principle and requested to minimize the total energy

$$E_{\text{HF}} = \min_{\{\varphi_k\}} \langle S\{\varphi_k\} | \hat{\mathcal{H}} | S\{\varphi_k\} \rangle$$

for a given number of particles \mathcal{N} . This yields the following equations for $\{\varphi_k\}$:

$$(\hat{h}_{\mathbf{k}} + \hat{V}) |\varphi_k\rangle = \varepsilon_k |\varphi_k\rangle, \quad (2)$$

where $\hat{h}_{\mathbf{k}} \equiv \|h_{\mathbf{k}}^{\alpha\beta}\|$ is the kinetic part of the model Hamiltonian (1) in the reciprocal space: $h_{\mathbf{k}}^{\alpha\beta} = \frac{1}{N} \sum_{\mathbf{R}, \mathbf{R}'} h_{\mathbf{R}\mathbf{R}'}^{\alpha\beta} e^{-i\mathbf{k} \cdot (\mathbf{R} - \mathbf{R}')}$ (N being the number of sites), and $\hat{V} \equiv \|V_{\alpha\beta}\|$ is the HF potential:

$$V_{\alpha\beta} = \sum_{\gamma\delta} (U_{\alpha\beta\gamma\delta} - U_{\alpha\delta\gamma\beta}) n_{\gamma\delta}. \quad (3)$$

In the following, we will also use the notation \hat{h}_{HF} , which stands for the total Hamiltonian of the HF method, $\hat{h} + \hat{V}$. Eq. (2) is solved self-consistently together with the equation

$$\hat{n} = \sum_k^{\text{occ}} |\varphi_k\rangle \langle \varphi_k|$$

for the density matrix $\hat{n} \equiv \|n_{\alpha\beta}\|$ in the basis of Wannier orbitals. Finally, the total energy in the HF method can be obtained as

$$E_{\text{HF}} = \sum_k^{\text{occ}} \varepsilon_k - \frac{1}{2} \sum_{\alpha\beta} V_{\beta\alpha} n_{\alpha\beta}.$$

3.2. Second Order Perturbation Theory for Correlation Energy

The simplest way to go beyond the HF approximation is to include the correlation interactions in the second order of perturbation theory for the total energy [13]. The correlation interaction (or a fluctuation) is defined as the difference between true many-body Hamiltonian (1), and its one-electron counterpart, obtained at the level of HF approximation:

$$\hat{\mathcal{H}}_C = \sum_{\mathbf{R}} \left(\frac{1}{2} \sum_{\alpha\beta\gamma\delta} U_{\alpha\beta\gamma\delta} \hat{c}_{\mathbf{R}\alpha}^\dagger \hat{c}_{\mathbf{R}\gamma}^\dagger \hat{c}_{\mathbf{R}\beta} \hat{c}_{\mathbf{R}\delta} - \sum_{\alpha\beta} V_{\alpha\beta} \hat{c}_{\mathbf{R}\alpha}^\dagger \hat{c}_{\mathbf{R}\beta} \right). \quad (4)$$

By treating $\hat{\mathcal{H}}_C$ as a perturbation, the correlation energy can be easily estimated as [13]:

$$E_C^{(2)} = - \sum_S \frac{\langle G | \hat{\mathcal{H}}_C | S \rangle \langle S | \hat{\mathcal{H}}_C | G \rangle}{E_{\text{HF}}(S) - E_{\text{HF}}(G)}, \quad (5)$$

where $|G\rangle$ and $|S\rangle$ are the Slater determinants corresponding to the low-energy ground state in the HF approximation, and the excited state, respectively. Due to the variational properties of the HF method, the only processes which may contribute to $E_C^{(2)}$ are the two-particle excitations, for which each $|S\rangle$ is obtained from $|G\rangle$ by replacing two one-electron orbitals, say φ_{k_1} and φ_{k_2} , from the occupied part of the spectrum by two unoccupied orbitals, say φ_{k_3} and φ_{k_4} . Hence, using the notations of Sec. 2., the matrix elements take the following form:

$$\langle S | \hat{\mathcal{H}}_C | G \rangle = \langle k_3 k_4 | v_{\text{scr}} | k_1 k_2 \rangle - \langle k_3 k_4 | v_{\text{scr}} | k_2 k_1 \rangle. \quad (6)$$

Then, we employ a common approximation of noninteracting quasiparticles and replace the denominator of Eq. (5) by the linear combination of HF eigenvalues: $E_{\text{HF}}(S) - E_{\text{HF}}(G) \approx \varepsilon_{k_3} + \varepsilon_{k_4} - \varepsilon_{k_1} - \varepsilon_{k_2}$ [13]. The matrix elements (6) satisfy the following condition: $\langle S | \hat{\mathcal{H}}_C | G \rangle \sim \frac{1}{N} \sum_{\mathbf{R}} e^{i(\mathbf{k}_3 + \mathbf{k}_4 - \mathbf{k}_1 - \mathbf{k}_2) \cdot \mathbf{R}}$, provided that the screened Coulomb interactions are diagonal with respect to the site indices.

A good point of the second-order of the perturbation theory is that it allows us to estimate relatively easily both on-site ($\mathbf{R}=0$) and intersite ($\mathbf{R} \neq 0$) elements

of this expansion. In the following, we will use this method in order to study the relative role played by these effects in the stability of different magnetic structures of the distorted perovskite oxides. The $\mathbf{R}=0$ term corresponds to the commonly used single-site approximation for the correlation interactions, which becomes exact in the limit of infinite spacial dimensions [19].

3.3. *t*-matrix approach

The basic idea of the *t*-matrix approach is to look at the true many-electron system as a superposition of independent two-electron subsystems, and to solve rigorously the Schrödinger equations for each of these subsystems [14, 15, 16]. Hence, we consider the following two-electron Hamiltonian:

$$\hat{H}(1, 2) = \hat{h}_{\text{HF}}(1) + \hat{h}_{\text{HF}}(2) + \Delta\hat{v}(1, 2),$$

where $\Delta\hat{v}(1, 2) = \hat{v}_{\text{scr}}(1, 2) - \hat{V}(1) - \hat{V}(2)$, $\hat{v}_{\text{scr}}(1, 2)$ is the screened (by other bands) Coulomb interactions between electrons ‘1’ and ‘2’ in the t_{2g} band, and \hat{h}_{HF} (\hat{V}) is the one-electron Hamiltonian (potential) in the HF approximation. For the periodic system, the Schrödinger equation can be written in the following form:

$$\hat{H}|\Psi_{k_1 k_2}\rangle = E_{k_1 k_2}|\Psi_{k_1 k_2}\rangle. \quad (7)$$

Any two-electron wavefunction $|\Psi_{k_1 k_2}\rangle$ can be expanded in the basis of (also two-electron) Slater’s determinants: $|k_1 k_2\rangle = \frac{1}{\sqrt{2}}\{\varphi_{k_1}(1)\varphi_{k_2}(2) - \varphi_{k_2}(1)\varphi_{k_1}(2)\}$, etc. Apart from a normalization multiplier, this expansion has the following form [16]:

$$|\Psi_{k_1 k_2}\rangle = |k_1 k_2\rangle + \sum_{|k_3 k_4\rangle} \Gamma_{k_1 k_2}^{k_3 k_4} |k_3 k_4\rangle. \quad (8)$$

Note that the summation goes only over *nonequivalent* Slater’s determinant $|k_3 k_4\rangle$, constructed from the one-electron orbitals k_3 and k_4 . For example, since $|k_4 k_3\rangle = -|k_3 k_4\rangle$, the determinant $|k_4 k_3\rangle$ should be excluded from the sum (8), etc. By substituting Eq. (8) into Eq. (7), and introducing the new notations $\Delta E_{k_1 k_2} = E_{k_1 k_2} - \varepsilon_{k_1} - \varepsilon_{k_2}$, such that

$$[\hat{h}_{\text{HF}}(1) + \hat{h}_{\text{HF}}(2) - \varepsilon_{k_1} - \varepsilon_{k_2}] |k_1 k_2\rangle = 0$$

(i.e., ε_{k_1} and ε_{k_2} are the eigenvalues of the HF Hamiltonian), one obtains the following equation for $\Delta E_{k_1 k_2}$ and $\Gamma_{k_1 k_2}^{k_3 k_4}$:

$$(\Delta\hat{v} - \Delta E_{k_1 k_2}) |k_1 k_2\rangle + \sum_{|k_3 k_4\rangle} (\varepsilon_{k_3} + \varepsilon_{k_4} - \varepsilon_{k_1} - \varepsilon_{k_2} + \Delta\hat{v} - \Delta E_{k_1 k_2}) \Gamma_{k_1 k_2}^{k_3 k_4} |k_3 k_4\rangle = 0.$$

By considering the matrix element of this equation with $\langle k_1 k_2|$, one can find that

$$\Delta E_{k_1 k_2} = \langle k_1 k_2 | \Delta\hat{v} | k_1 k_2 \rangle + \sum_{|k_3 k_4\rangle} \Gamma_{k_1 k_2}^{k_3 k_4} \langle k_1 k_2 | \Delta\hat{v} | k_3 k_4 \rangle, \quad (9)$$

where the first term is the energy of Coulomb and exchange interactions in the HF approximation (minus the potential energy), while the second term is the correlation

energy. By considering the matrix elements with $\langle k_5 k_6 | \neq \langle k_1 k_2 |$, one can find another set of equations for $\Gamma_{k_1 k_2}^{k_3 k_4}$.

$$\langle k_5 k_6 | \Delta \hat{v} | k_1 k_2 \rangle + (\varepsilon_{k_5} + \varepsilon_{k_6} - \varepsilon_{k_1} - \varepsilon_{k_2} - \Delta E_{k_1 k_2}) \Gamma_{k_1 k_2}^{k_5 k_6} + \sum_{|k_3 k_4\rangle} \Gamma_{k_1 k_2}^{k_3 k_4} \langle k_5 k_6 | \Delta \hat{v} | k_3 k_4 \rangle = 0.$$

They are solved iteratively with respect to $\Delta \hat{v}$. In order to do so, it is convenient to introduce the two-particle Green's function,

$$\hat{G}_{k_1 k_2} = \sum_{|k_3 k_4\rangle} \frac{|k_3 k_4\rangle \langle k_3 k_4|}{\varepsilon_{k_3} + \varepsilon_{k_4} - \varepsilon_{k_1} - \varepsilon_{k_2} - \Delta E_{k_1 k_2}},$$

and derive a matrix equation for $\{\Gamma_{k_1 k_2}^{k_3 k_4}\}$, which are then substituted into Eq. (9). Then, it is rather straightforward to derive the following expression for $\Delta E_{k_1 k_2}$:

$$\Delta E_{k_1 k_2} = \langle k_1 k_2 | \hat{T}_{k_1 k_2} | k_1 k_2 \rangle, \quad (10)$$

where $\hat{T}_{k_1 k_2}$ is the so-called t -matrix:

$$\hat{T}_{k_1 k_2} = \Delta \hat{v} [\hat{1} + \hat{G}_{k_1 k_2} \Delta \hat{v}]^{-1}. \quad (11)$$

The correlation energy of the t -matrix method is obtained after the subtraction from Eq. (10) the energies of Coulomb and exchange interactions in the HF approximation and summation up over all Slater's determinants constructed from the occupied one-electron orbitals of the HF method:

$$E_C^{(t)} = \sum_{|k_1 k_2\rangle}^{occ} \langle k_1 k_2 | \hat{T}_{k_1 k_2} - \Delta \hat{v} | k_1 k_2 \rangle. \quad (12)$$

In practice, each HF orbital has been expanded over the basis of Wannier functions, and then all calculations of $\hat{T}_{k_1 k_2}$ and $E_C^{(t)}$ have been performed in this basis.

By expanding $\hat{T}_{k_1 k_2}$ up to the second order of $\Delta \hat{v}$, we regain Eq. (5), obtained in the second order of perturbation theory. Therefore, the good point of the t -matrix approach is that it allows us to go beyond the second order of perturbation theory and evaluate the higher order effects of $\Delta \hat{v}$ onto the correlations energy. Nevertheless, it was supplemented with some additional approximations.

1. When we compute the matrix elements of the form $\langle k_3 k_4 | \Delta \hat{v} | k_1 k_2 \rangle$, being proportional to $\frac{1}{N} \sum_{\mathbf{R}} e^{i(\mathbf{k}_3 + \mathbf{k}_4 - \mathbf{k}_1 - \mathbf{k}_2) \cdot \mathbf{R}}$, we consider only the $\mathbf{R} = 0$ part of this sum and neglect all other contributions. This corresponds to the single-site approximation for the t -matrix.
2. In all matrix elements $\langle k_3 k_4 | \Delta \hat{v} | k_1 k_2 \rangle$, we replace $\Delta \hat{v}$ by \hat{v}_{scr} and drop the one-electron potentials of the HF method. Strictly speaking, this procedure is justified only when both one-electron states k_1 and k_2 are different from k_3 and k_4 , for example, when they belong, correspondingly, to the occupied and unoccupied part of the spectrum, like in the second order of perturbation theory. However, this is no longer true for the higher-order terms with respect to $\Delta \hat{v}$. Nevertheless, we believe that the difference is small.

All correlation energies have been computed in the mesh of 75 points in the first Brillouin zone (BZ), corresponding to the 4:4:2 divisions of the reciprocal translation vectors for the distorted perovskite structure. The actual integration over the BZ has been replaced by the summation over this mesh of points.

4. Results and Discussions

First applications of the proposed method to YTiO_3 , LaTiO_3 , YVO_3 , and LaVO_3 have been considered in Ref. [11], where we have summarized results of HF calculations for the model (1) and the behavior of correlation energies in the second order of perturbation theory, supplemented with the single-site approximation. In the present work we will further elaborate the problem by focusing on the following question:

1. the role of higher-order contributions to the correlation energy;
2. the role of nonlocal (or intersite) contributions to the correlation energy.

We will also consider the effects of monoclinic distortion and analyze the contributions to the correlation energy of inequivalent transition-metal sites. The results of these calculations are presented in Tables 1-5 for all considered compounds. First, we would like to summarize the main results of Ref. [11].

1. The HF approximation yields the correct magnetic ground state for YTiO_3 , LaVO_3 , and both phases of YVO_3 . This conclusion is fully consistent with the results of accurate all-electron band-structure calculations [5], and this is quite remarkable that all these results can be reproduced in our minimal model derived for the t_{2g} bands.
2. The correlation effects favor the AFM spin alignment and additionally stabilize the experimentally observed G - and C -type AFM states in YVO_3 and LaVO_3 .
3. None of the considered approaches reproduces the experimental G -type AFM ground state of LaTiO_3 (instead, the theoretical calculations steadily converge to the A -type AFM ground state [11, 12]).

Then, what will happen if we go beyond the second-order perturbation theory and apply the t -matrix approach? Generally, the t -matrix approach reduces the absolute value of the correlation energy. However, the magnitude of this reduction strongly depends on the magnetic state. For example, if the F state is only weakly affected by the higher-order correlation effects (the typical changes of E_C varies from 1% in YVO_3 till 13% in LaTiO_3), E_C in the G -type AFM phase can drop by nearly 50%. From this point of view, if the second order or perturbation theory does not solve the problem of the G -type AFM ground state of LaTiO_3 , it seems to be unlikely that the higher-order effects can reverse the situation. Apparently, LaTiO_3 is different from other perovskite oxides, and the regular perturbation-theory expansion, though may be justified for the majority of considered compounds, does not work in the case of LaTiO_3 . This seems to be reasonable, because LaTiO_3 has the largest correlation energies, which are comparable with the splitting of the t_{2g} levels caused by the crystal distortion (~ 37 meV [11]). Therefore, it is quite possible that the correlation effects in LaTiO_3 should be considered *at the first place*, and the simple HF theory for the spin and orbital ordering with the subsequent inclusion of the correlation effects as a perturbation to the HF ground state may not be appropriate here [7, 8]. Note that in other materials, the situation is different: the typical values of the t_{2g} -levels splitting in YTiO_3 , YVO_3 , and LaVO_3 are about 100 meV [11], which exceeds the correlation energy by at least one order of magnitude. Therefore, it seems that

the degeneracy of the HF ground state is already lifted by the crystal distortion, and the correlation effects are well described by means of the regular perturbation theory expansion. This is partly supported by recent total energy calculations for the orthorhombic phase of YVO_3 using path-integral renormalization group method, which is free of any perturbation-theory expansions for the correlation energy [20]. The method was applied to the same model, and the main conclusions concerning the magnetic phase diagram were similar to our present finding.

The correlations additionally stabilize the experimentally observed G - and C -type AFM states in YVO_3 and LaVO_3 . Moreover, in the orthorhombic phase of YVO_3 , the correlation effects tend to stabilize the G -type AFM state; while in the monoclinic phase, they stabilize the C -type AFM state, being in total agreement with the experimental data. This trend is clearly seen both in the second order of perturbation theory and in the t -matrix approach, though the latter yield somewhat smaller values for the stabilization energy associated with the correlation effects.

The higher-order correlations play an important role in YTiO_3 and additionally stabilize the ferromagnetic phase. The latter emerges as the ground state already in the HF approach, where the total energy difference between ferromagnetic and the next A -type AFM state is about 2.05 meV per one Ti site (Table 1). However, if we take into account the correlation effects in the second order of perturbation theory (and consider the single-site approximation), this difference is reduced to only 0.99 meV. Therefore, the situation is very fragile. Nevertheless, the t -matrix approach, which affects more strongly the A -type AFM state, will recover some of these energy gains and make the total energy difference between ferromagnetic and A -type AFM states to be about 1.83 meV per one Ti site.

The intersite correlation energies, which have been estimated in the second order of perturbation theory, can be large in some ferromagnetically couple bonds. This is especially true for YTiO_3 and LaVO_3 . For example, the energy of interaction between nearest-neighbor sites ‘1’ and ‘2’ (see Fig. 1), located in the **ab**-plane of the ferromagnetic phase of YTiO_3 is about -0.38 meV (Table 1). Since in the **ab**-plane, each transition-metal atom interacts with four nearest neighbors, it corresponds to the additional energy gain $-0.38 \times 4 = -1.52$ meV per one Ti site. Similar estimates yield $-0.37 \times 4 = -1.48$ meV, $-0.17 \times 4 = -0.68$ meV, and $-0.18 \times 4 = -0.72$ meV, correspondingly for the A -, C -, and G -type AFM states. Therefore, the in-plane intersite correlations tend to additionally stabilize the ferromagnetic phase relative to the AFM states C and G . In the A -type AFM phase, the sites ‘1’ and ‘2’ are also ferromagnetically coupled, like in the totally ferromagnetic phase. Therefore, these two phases have practically the same intersite correlation energies in the **ab**-plane. The inter-plane correlations appear to be small in all magnetic phases of YTiO_3 .

In LaVO_3 , the situation is somewhat different, and this is a good example of the system where already the inter-plane correlations play a more important role. Indeed, the energies of intersite correlations are the largest in the ferromagnetic chains of C -type AFM phase, which is also the magnetic ground state of this compound. These energies are associated with the bonds ‘1-3’ and ‘2-4’, which are shown in Fig. 1, and the results are summarized in Table 4. Thus, in the case of LaVO_3 , the inter-plane correlations additionally stabilize the C -type AFM ground state. However, since each transition-metal atom interacts with only two nearest neighbors along the **c** axis, the stabilization energy is not particularly large (about $-0.26 \times 2 = -0.52$ meV per one V atom).

The intersite correlation energies are large also in the case of LaTiO_3 (Table 5). However, they tend to stabilize either ferromagnetic or *A*-type AFM states, and do not explain the appearance of experimental *G*-type AFM ground state. Again, we believe that the problem is related with the use of the regular perturbation theory expansion, which may not be justified in the case of LaTiO_3 .

The monoclinic distortion realized in LaVO_3 and in the high-temperature phase of YVO_3 produces two inequivalent pairs of transition-metal sites, which are shown correspondingly as (1,2) and (3,4) in Fig. 1. Therefore, it is interesting to consider the interplay between correlation energies and the lattice distortions around different transition-metal sites. In our notations, the crystal structure around the sites ‘3’ and ‘4’ is more distorted than the one around the sites ‘1’ and ‘2’. Such a distortion directly correlates with the magnitude of the crystal-field splitting in different sublattices [11]. Then, the on-site correlations are generally stronger at the sites with the least distorted environment (site ‘1’ in the Tables 3 and 4). This rule holds both for YVO_3 and LaVO_3 (though with some exception for the ferromagnetic phase of LaVO_3). In the *C*-type AFM phase, which is always realized as the magnetic ground state in the monoclinic structure, the difference of on-site correlation energies associated with the sites ‘1’ and ‘4’ is about 1 meV per one V site, as obtained in the second order of perturbation theory. This value is further reduced till 0.5 meV per one V site by higher-order correlations in the *t*-matrix theory.

5. Summary and Conclusions

This paper is the continuation of previous works (Refs. [10], [11], and [12]) devoted to the construction and solution of an effective low-energy models for the series of distorted t_{2g} perovskite oxides on the basis of first-principles electronic structure calculations. It deals with the analysis of correlation interactions and their contributions to stability on different magnetic structures, which can be realized in these compounds. The correlation energies have been calculated on the basis of a regular perturbation theory expansion starting from the ground state of the HF method. Thus, our strategy implies that the degeneracy of the HF ground state is already lifted by the crystal distortion and the regular perturbation theory is justified. This seems to be a good approximation for the most distorted YTiO_3 , YVO_3 , and even LaVO_3 , where

1. the correct magnetic ground state can be formally obtained at the level of HF approximation;
2. the correlation effects, included as a perturbation to the HF ground state, systematically improve the agreement with the experimental data.

However, in LaTiO_3 , the situation is completely different:

1. the HF method yields an incorrect magnetic ground state (*A*-type AFM instead of *G*-type AFM);
2. the correlation interactions, treated as a perturbation to this incorrect HF ground state, do not change the overall picture, and the *G*-type AFM state remains unstable relative to the *A* state.

Thus, the origin of the G -type AFM ground state in LaTiO_3 seems to be different from other perovskite oxides and remains a challenging problem for future theories. Apparently, one of our basic assumptions about the nondegeneracy of the HF ground state breaks down in the case of LaTiO_3 , and the true ground state cannot be approached through the series of continuous corrections applied to the single-Slater-determinant HF theory. Therefore, the next important step for LaTiO_3 would be get rid of this “nondegeneracy assumption” and expand the class of the possible ground states, which would include some aspects of the orbital liquid theory [7].

ACKNOWLEDGMENTS

This work has been partially supported by Grant-in-Aids for Scientific Research in Priority Area “Anomalous Quantum Materials” from the Ministry of Education, Culture, Sports, Science and Technology of Japan.

References

- [1] D. A. Maclean, H.-N. Ng, and J. E. Greedan, *J. Solid State Chem.* **30**, 35 (1979); M. Itoh, M. Tsuchiya, H. Tanaka, and K. Motoya, *J. Phys. Soc. Jpn.* **68**, 2783 (1999); J. Akimitsu, H. Ichikawa, N. Eguchi, T. Miyano, M. Nishi, and K. Kakurai, *ibid.* **70**, 3475 (2001); C. Ulrich, G. Khaliullin, M. Reehuis, *et al.*, *Phys. Rev. Lett.* **89**, 167202 (2002); F. Iga, M. Tsubota, M. Sawada, *et al.*, *ibid.* **93**, 257207 (2004).
- [2] B. Keimer, D. Casa, A. Ivanov, *et al.*, *Phys. Rev. Lett.* **85**, 3946 (2000); M. Cwik, T. Lorenz, J. Baier, *et al.*, *Phys. Rev. B* **68**, 060401(R) (2003).
- [3] Y. Ren, T. T. M. Palstra, D. I. Khomskii, *et al.*, *Nature* **396**, 441 (1998); G. R. Blake, T. T. Palstra, Y. Ren, A. A. Nugroho, and A. A. Menovsky, *Phys. Rev. B* **65**, 174112 (2002); A. A. Tsvetkov, F. P. Mena, P. H. M. van Loosdrecht, *et al.*, *ibid.* **69**, 075110 (2004); C. Ulrich, G. Khaliullin, J. Sirker, *et al.*, *Phys. Rev. Lett.* **91**, 257202 (2003).
- [4] V. G. Zubkov, G. V. Bazuev, V. A. Perelyaev, and G. P. Shveikin, *Sov. Phys. Solid State* **15**, 1079 (1973); P. Bordet, C. Chaillout, M. Marezio, *et al.*, *J. Solid State Chem.* **106**, 235 (1993).
- [5] H. Sawada and K. Terakura, *Phys. Rev. B* **58**, 6831 (1998); Z. Fang and N. Nagaosa, *Phys. Rev. Lett.* **93**, 176404 (2004).
- [6] M. Mochizuki and M. Imada, *Phys. Rev. Lett.* **91**, 167203 (2003); R. Schmitz, O. Entin-Wohlman, A. Aharony, A. B. Harris, and E. Müller-Hartmann, *Phys. Rev. B* **71**, 144412 (2005).
- [7] G. Khaliullin and S. Maekawa, *Phys. Rev. Lett.* **85**, 3950 (2000).
- [8] G. Khaliullin and S. Okamoto, *Phys. Rev. Lett.* **89**, 167201 (2002); P. Horsch, G. Khaliullin, and A. M. Oleś, *ibid.* **91**, 257203 (2003).
- [9] Y. Imai, I. Solovyev, and M. Imada, *Phys. Rev. Lett.* **95**, 176405 (2005).
- [10] I. V. Solovyev, *Phys. Rev. B* **73**, 155117 (2006).
- [11] I. V. Solovyev, *Phys. Rev. B* **74**, 054412 (2006).
- [12] I. V. Solovyev, *Phys. Rev. B* **69**, 134403 (2004).
- [13] J. Friedel and C. M. Sayers, *J. Physique* **38**, 697 (1977); F. Kajzar and J. Friedel, *ibid.* **39**, 397 (1978); G. Treglia, F. Ducastelle, and D. Spanjaard, *ibid.* **41**, 281 (1980).
- [14] K. A. Brueckner and C. A. Levinson, *Phys. Rev.* **97**, 1344 (1955).
- [15] V. M. Galitskii, *J. Exp. Theor. Phys. (USSR)* **34**, 151 (1958).
- [16] J. Kanamori, *Prog. Theor. Phys.* **30**, 275 (1963).
- [17] I. V. Solovyev, Z. V. Pchelkina, and V. I. Anisimov, cond-mat/0608528.
- [18] O. K. Andersen, *Phys. Rev. B* **12**, 3060 (1975); O. K. Andersen, Z. Pawłowska, and O. Jepsen, *ibid.* **34**, 5253 (1986).
- [19] A. Georges, G. Kotliar, W. Krauth, and M. J. Rozenberg, *Rev. Mod. Phys.* **68**, 13 (1996).
- [20] Y. Otsuka and M. Imada, to be published.

Table 1: Hartree-Fock, E_{HF} , and correlation energies obtained in the second order of perturbation theory, $E_C^{(2)}$, and in the t -matrix approach, $E_C^{(t)}$, for the orthorhombic phase of YTiO_3 . The Hartree-Fock energies are measured from the most stable magnetic state in meV per one formula unit. The correlation energies are measured in meV per one transition-metal site or a pair of sites, correspondingly for the on-site and intersite contributions. Note that the t -matrix was computed in the single-site approximation. Therefore, only the site-diagonal part of $E_C^{(t)}$ is shown. The positions of the transition-metal sites are shown in Fig. 1.

Phase	E_{HF}	$E_C^{(2)}$			$E_C^{(t)}$
		Ti ₁	Ti ₁ -Ti ₂	Ti ₁ -Ti ₃	Ti ₁
<i>F</i>	0	-5.13	-0.38	-0.01	-4.58
<i>A</i>	2.05	-6.19	-0.37	0	-4.80
<i>C</i>	14.40	-8.32	-0.17	-0.01	-5.28
<i>G</i>	16.25	-8.48	-0.18	-0.01	-5.31

Table 2: Hartree-Fock, E_{HF} , and correlation energies obtained in the second order of perturbation theory, $E_C^{(2)}$, and in the t -matrix approach, $E_C^{(t)}$, for the low-temperature orthorhombic phase of YVO_3 ($T < 77$ K). All energies are measured in meV. See Fig. 1 for the details of the notations.

Phase	E_{HF}	$E_C^{(2)}$			$E_C^{(t)}$
		V_1	V_1-V_2	V_1-V_3	V_1
F	21.66	-2.19	-0.12	-0.02	-2.16
A	14.59	-4.67	-0.12	-0.01	-3.31
C	10.14	-5.61	-0.07	0	-3.14
G	0	-7.07	-0.07	-0.01	-4.06

Table 3: Hartree-Fock, E_{HF} , and correlation energies obtained in the second order of perturbation theory, $E_C^{(2)}$, and in the t -matrix approach, $E_C^{(t)}$, for the high-temperature monoclinic phase of YVO_3 ($77 \text{ K} < T < 116 \text{ K}$). All energies are measured in meV. See Table 1 for the details of the notations. Note that, in the monoclinic phase, the planes 1-2 and 3-4 are inequivalent (see Fig. 1). Therefore, there are two different types of on-site (denoted as V_1 and V_4) and intersite (denoted as V_1 - V_2 and V_4 - V_3) contributions to the correlation energy. The contributions V_1 - V_3 and V_4 - V_2 are equivalent and are both shown only for the sake of completeness.

Phase	E_{HF}	$E_C^{(2)}$						$E_C^{(t)}$	
		V_1	V_1 - V_2	V_1 - V_3	V_4	V_4 - V_3	V_4 - V_2	V_1	V_4
F	11.71	-2.81	-0.02	-0.03	-1.74	-0.01	-0.03	-2.76	-1.71
A	13.97	-5.87	-0.03	-0.01	-3.63	-0.01	-0.01	-4.14	-2.55
C	0	-8.08	-0.02	-0.05	-6.98	-0.03	-0.05	-4.85	-4.33
G	6.63	-7.56	-0.02	-0.01	-6.49	-0.03	-0.01	-4.38	-3.76

Table 4: Hartree-Fock, E_{HF} , and correlation energies obtained in the second order of perturbation theory, $E_C^{(2)}$, and in the t -matrix approach, $E_C^{(t)}$, for the monoclinic phase of LaVO_3 . All energies are measured in meV. See Tables 1 and 3 for the details of the notations. Note that, in the monoclinic phase, the planes 1-2 and 3-4 (see Fig. 1) are inequivalent, that results in two types of V sites as well as the in-plane interactions.

Phase	E_{HF}	$E_C^{(2)}$						$E_C^{(t)}$	
		V_1	V_1 - V_2	V_1 - V_3	V_4	V_4 - V_3	V_4 - V_2	V_1	V_4
F	20.98	- 3.82	-0.02	-0.15	- 4.13	-0.02	-0.15	-3.74	-4.02
A	20.63	-11.77	-0.22	-0.03	- 8.80	-0.02	-0.03	-8.34	-5.84
C	0	-13.37	-0.04	-0.26	-12.54	-0.02	-0.26	-8.86	-8.39
G	7.65	-10.52	-0.04	-0.02	- 9.02	-0.03	-0.02	-6.17	-5.41

Table 5: Hartree-Fock, E_{HF} , and correlation energies obtained in the second order of perturbation theory, $E_C^{(2)}$, and in the t -matrix approach, $E_C^{(t)}$, for the orthorhombic phase of LaTiO_3 . All energies are measured in meV. See Table 1 for the details of the notations.

Phase	E_{HF}	$E_C^{(2)}$			$E_C^{(t)}$
		Ti ₁	Ti ₁ -Ti ₂	Ti ₁ -Ti ₃	Ti ₁
F	4.95	-11.08	-0.52	-0.08	- 9.66
A	0	-22.53	-0.54	-0.07	-15.17
C	19.57	-17.19	-0.23	-0.11	-11.04
G	11.51	-23.02	-0.22	-0.09	-13.99

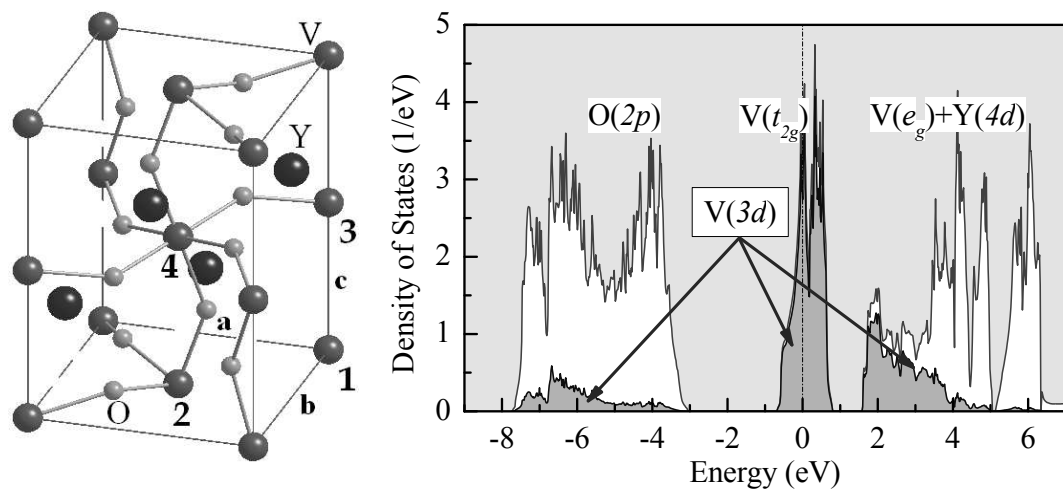


Figure 1: A characteristic example of the crystal structure (left) and the electronic structure in the local-density approximation (right) of the orthorhombically distorted YVO_3 . In the left panel, the symbols **a**, **b**, and **c** stand for orthorhombic translations, and the symbols 1–4 denote the transition-metal sites, which form the unit cell of the distorted perovskite oxides. In the right panel, the shaded area shows contributions of the atomic $\text{V}(3d)$ states. Other symbols show the positions of the main bands. The Fermi level is at zero energy.